DETECTION OF RECENT FAULTING AND EVALUATION OF THE VERTICAL OFFSETS FROM NUMERICAL ANALYSIS OF SAR-ERS-1 IMAGES. THE EXAMPLE OF THE ATACAMA FAULT ZONE IN NORTHERN CHILE.

Catherine MERING[1][2] Jean CHOROWICZ[2][3], Jean Claude VICENTE[3] and Cherif CHALAH[3]

[1] ORSTOM, 213 rue Lafayette 75010 Paris. France.

(2) URA 1759 CNRS, UPMC, Case 129-T26E1. 4 Place Jussieu

F 75252 Paris Cedex 05, e-mail: mering@ulysse.lgs.jussieu.fr

(3) Département de Géotectonique, UPMC, 4 Place Jussieu, F 75252 Paris Cedex 05

KEYWORDS: CHILE, IMAGE ANALYSIS, RADAR IMAGERY, TECTONICS

TOPOGRAPHIC EFFECT OF RECENT FAULT SCARPS ON RADAR SAR IMAGES

Its is already well known that the relationship between the antenna depression angle of the incident beam and the surface slope of macro-scale features is very significant in the interpretation of radar images.

The foreslopes of topographic features (slopes facing the antenna) are responsible for strong echoes with the greatest amount of reflection occuring when the local slope is perpendicular to the radar beam (Ulaby et al., 1982), which corresponds to a 67°C angle in the case of SAR ERS-1 images. This condition, known as normal incidence, produces a very bright area on the image. Abrupt scarps such as those of recent faults (see Fig. 1) which face radar illumination can be then considered as creating conditions for such a foreslope brightening .

Besides, the presence of topographic relief in a scene can introduce distorsions known as *foreshortening* and *layover*. We will see whether the specific conditions of the viewing on fault scarps are affected by these distorsions.

With radar imaging, all foreslopes are shortened relatively to their true lengths (Fig. 1). The degree of shortening is a function of the illumination geometry and the foreslope angle acording to the equation (1):

$$A'B = AB\cos\alpha^{+}\left(1 - \tan\alpha^{+}/\tan\theta\right)\sin\theta \quad (1)$$

where α^+ is the foreslope angle and θ is the look angle.

The greater the foreshortening, the more energy per unit area is displayed on the image until so much is avalaible that it saturates the reciever.

Besides, *layover* is an extreme case of foreshortening that occurs whenever the look angle is smaller than the fore slope angle. In this situation, the echo from the foreslope summit will be recieved first because the slant range is shorter to the top of the feature than it is to the base.. In this case a topographic feature will appear to be laid over on its side towards the near range. (Fig.1). The layover occurs mainly when steep slopes are encountered in the near range (Franceschetti et al., 1994).

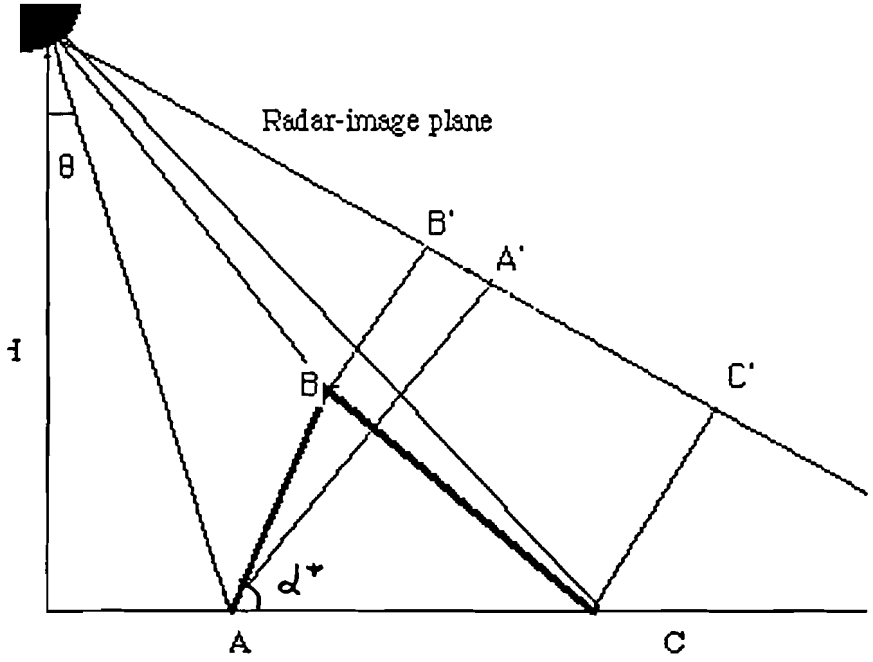

Figure 1

We suppose here that the slope AB on Figure 1 corresponds to the part of the fault plane where the slope angle is constant. The foreshortening effect will then be constant for the corresponding range A'B' on the image. The lower and the upper parts of the versant are affected by erosion so that their slope angles are smaller and their radiometry will be lower than that of the middle part AB.

ANALYSIS OF THE RADAR SCENE OF THE ATACAMA FAULT ZONE

The training zone is situated here on segments of the Atacama fault in Northern Chile. In late Miocene, the Atacama Fault Zone (AFZ) has suffered major neotectonic reactivation and deformation continues until Present (Armijo and Thiele, 1991).

The SAR ERS-1 scenes were acquired on 02 June 1992, from an orbit 785 km in altitude, using an antenna inclined 23° off nadir operating in the C-band (5.3 Ghz). The observed earth surface is 100 by 100 km and ground resolution is 12,5 m .We show on figure 2 a segment of the fault from a subscene of a Radar SAR ERS-1 image.

Most of the segments of the AFZ are oriented NW-SE (Okada, 1972) and are consequently sub orthogonal to the radar beam. Within such a context, it is obvious that radar SAR ERS-1 images significantly enhances the mapping of this fault system. Recent faults corresponds thence to white lineaments on the image.

This type of fault is characterized by changes in the scarp height along the strike which corresponds on the image to variations of the thickness of the fault line (see Fig 2). In this case, we suppose that the fault dip is constant and that only the scarp height varies. The foreshortening effect must consequently be constant along the scarp and the fault line appears as a light line, the width of which beeing proportional to the slope length and therefore to the scarp height.

It is then possible to estimate relative fault throws along the same fault line, by calculating the width of the line on the radar image.

The features to extract correspond to sharp white lines on the radar image (Chorowicz et. al., 1993). The extraction is achieved by an image filtering reducing speckle noise called the connected center filter β_c (Mering and Parrot, 1994) followed by a high tresholding. The white components still remaining on the image.being thinner than the object to exctract are eliminated by a *Geodesic Reconstruction* (Serra, 1988), while thicker ones are eliminated after a labelling (Fig.3).

EVALUATION OF VERTICAL OFFSETS

The thickness of the line corresponding to the fault scarp is calculated by an image transformation called the *distance function* (Daniellson, 1980) which provides for each pixel of any connected component, a grey tone value which corresponds to a numeric distance between the pixel and the edge of the component . Such a *distance function* is used here to evaluate the thickness of irregular shapes on binary images. The *Maximal Thickness* of a connected component is then obtained by propagation of the highest value of the *distance function* inside each component. It provides an image on which each pixel has the numering value of the Maximal Thickness inside the connected component. (Fig. 4).

The result of computation of the *distance function* on the binary image (Fig. 3) gives 12 pixels as the value for the *Maximal Thickness*. From computation of the thickness of the lines which correspond to the A'B' in equation (1), we can deduce an estimation of the vertical fault throw h, knowing that:

$$h = AB \sin \alpha^{+}$$

The vertical fault throw h along the fault line. was calculated from a value of 12,5 meters for the pixel of the ERS-1 scene, and from a A'B' displacement value on the image of 8 pixels, which corresponds to one component on the example shown on Figure 4.

According to recent measurements on the ground, the slope along the scarp on this fault segment is about 77° (Gonzales et al, 1996). We conclude therefore that, taking into account both the *layover* and the *foreshortening*, effects on ERS-1 image, the fault throw at this place of the fault, can be estimated in this case as 120 meters high, from image analysis.

REFERENCES

Armijo R. and Thiele H., 1990. Active faulting in Northern Chile: Ramp stacking and Lateral Decoupling along a Subduction Plate Boundary. *Earth Planet. Sci. Lett.*, vol 98, 1990, pp40-61

Chorowicz J., Deffontaines B., Huaman-Rodrigo H., Luxey P., Pubellier and J.P. Rudant, 1993 Geomorphic objects detected by ERS1-SAR images in different geodynamic contexts. *Proceedings of Second ERS-1 Symposum Space at the Service of our Environment*, Hamburg, Germany, 11-14 October 1993, pp923-929.

Daniellson P.E., 1980, Euclidian Distance Mapping, *Computer Graphics and Image Processing*, vol14, pp227-248.

Dewey J.F. and Lamb S.H. , 1992. Active tectonics of the Andes, *Tectonophysics, vol 205*, pp 79-95.

Franceschetti G,.Marino R., Migliaccio M. and Riccio D. On SAR simulation on three-dimensional scenes. SPIE, Vol 2316, *SAR Data Processing for Remote Sensing*, 1994, pp192-198.

Gonzales L.G., Niemeyer H., Martinez E., 1996. Evolucion Tectonica Cenozoica del bordo continental en las immediaciones de Antofagasta: su relacion con la sedimentacion y la morfologia. Revista Geol. de Chile (in press).

Mering C. and Parrot J.F., 1994. Radar image analysis using morphological filters. *Mathematical Morphology and its Applications to Signal Processing*, eds J. Serra and P. Soille, Kluwer Academic Publisher, pp353-360.

Okada A. , 1972. On the neotectonics of the Atacama region. Preliminary notes on Late Cenozoic Faulting and geomorphic development of the Coast range of Northern Chile. *Bull. Dept Geography, Univ. Tokyo*, v3, pp47-65.

Serra J., 1988. Image Analysis and Mathematical Morphology. Vol. 2, Theoritical Advances, Academic Press, London, 411 p.

Ulaby F.T., Moore R.K and Fung A.K., 1982. Microwave Remote Sensing, vol 2, *Archtech House Inc.*

Figure 2: ERS-1 subscene of the Atacama Fault Zone

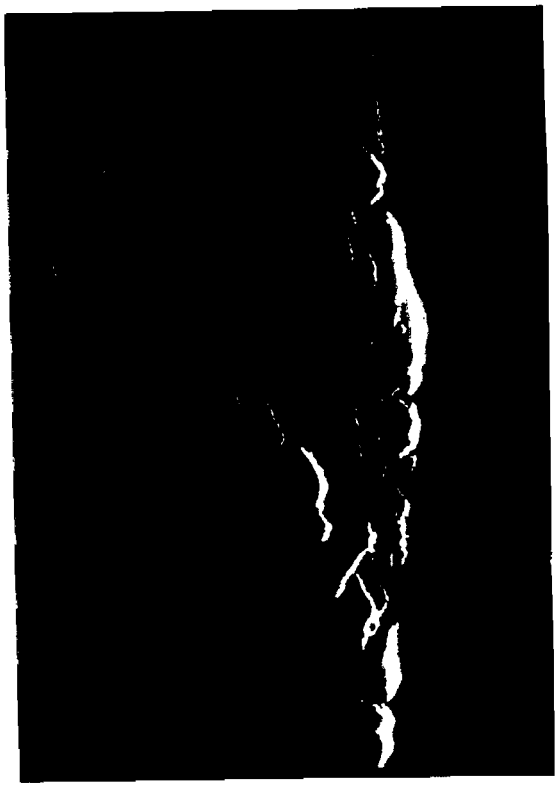

Figure 3: Extraction of fault scarps

Figure 4: Maximal Thickness image